JOURNAL OF CATALYSIS 132, 145–156 (1991)

Adsorption Sites on Pd/Al_2O_3

EDWARD C. HSIAO AND JOHN L. FALCONER

Department of Chemical Engineering, University of Colorado, Boulder, Colorado 80309-0424

Received February 5, 1991; revised June 13, 1991

On a Pd/Al_2O_3 catalyst, CO and H_2 interact to form CH_3O on the Al_2O_3 support. This CH_3O hydrogenates to CH_4 at a faster rate than the CO adsorbed on Pd. At high CH_3O coverages, CH_3O decomposition competes with hydrogenation. The effects of H_2 pressure and adsorption temperature on the rate of CH_3O formation were measured. Isotope studies show that CO adsorbs on Pd and then spills over onto Al_2O_3 where CH_3O is more readily hydrogenated to CH_4. The higher methanation activity of CH_3O than of CO on Pd may be responsible for the much higher, steady-state methanation activity observed for Pd/Al_2O_3 than for Pd/SiO_2 catalysts.

INTRODUCTION

When CO and H_2 coadsorb on Al_2O_3- and TiO_2-supported metals (Ni, Ru, Pt) at elevated temperatures, CO and H_2 adsorb directly on the metal and also form a CH_xO species on the support by spillover. Temperature-programmed reaction (TPR) has shown that these two adsorbed species hydrogenate to CH_4 at different rates. On Ni/Al_2O_3 (*1–4*), Ni/TiO_2 (*5*), and Ru/Al_2O_3 (*6*) catalysts, CO adsorbed on the metal is hydrogenated to CH_4 faster than CH_xO is hydrogenated. In contrast, on Pt/Al_2O_3 (*7, 8*) and Pt/TiO_2 (*9*) catalysts, the CH_xO species is hydrogenated faster than CO adsorbed on Pt. On Pt/Al_2O_3 (*7*), the CH_xO species was shown by infrared spectroscopy to be methoxy (CH_3O). On all these catalysts, the stoichiometry of CH_xO, as measured by temperature-programmed desorption (TPD), was close to that of a CH_3O species. The Ni, Ru, and Pt catalysts exhibit different behaviors because Pt is a poor methanation catalyst, but Ni and Ru are active methanation catalysts.

On Pd/SiO_2 and unsupported Pd catalysts, steady-state methanation activity is low, but the activity of Pd/Al_2O_3 is 70-fold greater than unsupported Pd and 35 times that of Pd/SiO_2 (*10*). Thus, the specific activities of Pd/Al_2O_3 catalysts were only a factor of three less than those of typical Ni methanation catalysts (*10*).

Since infrared spectroscopy has observed a CH_3O species adsorbed on the support of Pd/Al_2O_3, but not on Pd/SiO_2 upon exposure to H_2/CO mixtures (*11*), hydrogenation of CH_3O may be responsible for the higher methanation activity of Pd/Al_2O_3. On Ni catalysts, CO dissociates at relatively low temperatures and thus Ni is an active methanation catalyst. In contrast, CO does not dissociate as readily on Pd (*11*), and CO dissociation to carbon and oxygen may not be the pathway followed to form CH_4 on Pd. The objective of the present study was to measure the rate of CH_3O formation and hydrogenation on Pd/Al_2O_3. Temperature-programmed reaction was used to measure the hydrogenation rate, and TPD was used to determine if CH_3O was present on the Pd/Al_2O_3 catalyst. TPD and TPR have only been used previously in a few studies to characterize supported Pd catalysts (*12–16*).

A Pd/Al_2O_3 catalyst might be expected to behave differently from supported Pt catalysts, however, since Pd is a selective methanol synthesis catalyst at higher pressures (*17*), and thus CH_3O might be expected to form more readily on the Pd surface. Since

0021-9517/91 $3.00

methanol forms only at higher pressures (*10, 17*), coadsorption was also carried out in 2.6 atm H_2 pressure in some experiments to try to increase the yield of methanol or methoxy.

EXPERIMENTAL METHODS

Temperature-programmed desorption (TPD) and reaction (TPR) experiments were carried out on a 3.7% Pd/Al_2O_3 catalyst in a modified version of an apparatus that was described previously (*1, 18*). A quartz frit, mounted in a 1-cm OD quartz downflow reactor, supported 100 mg of catalyst (60–80 mesh). The reactor was placed in an electric furnace with a 0.5-mm OD chromel-alumel shielded thermocouple centered in the catalyst bed. A temperature programmer used feedback from this thermocouple to raise the catalyst temperature from 300 to 773 K at a constant rate of 1 K/s. Immediately downstream from the reactor, the effluent gas was continuously analyzed by a UTI quadrupole mass spectrometer. A sampling valve interfaced the ambient-pressure gas stream to the ultrahigh vacuum system, which contained the mass spectrometer and was pumped by a turbomolecular pump. A computer allowed simultaneous observation of multiple masses and the thermocouple signal. For the TPD experiments, masses 2 (H_2), 15 (CH_3), 18 (H_2O), 28 (CO), and 44 (CO_2) were monitored. Methane was observed at mass 15 to avoid CO, CO_2, and H_2O cracking fractions at mass 16. In the TPR experiments, masses 15, 18, 28, 31 (CH_3O), 44, 45 (CH_3OCH_2), and 46 (CH_3OCH_3) were monitored. Mass 31 is the largest cracking fragment of CH_3OH. The mass 28 and 31 signals were corrected for CO_2 and CH_3OCH_3 cracking, respectively. Known volumes of pure gas or liquid were injected into the carrier gas, downstream of the reactor, to calibrate the mass spectrometer.

At the beginning of each series of experiments, the reduced catalyst was pretreated for 2 h at 773 K in ambient pressure H_2 flow. To maintain a clean surface, the catalyst was treated in H_2 at 773 K for 15 min after each TPR experiment. Carbon monoxide was adsorbed on the catalyst by using a pulse valve, which injected 0.15 cm^3 (STP) samples of 10% CO/90% He into the carrier gas twice a minute.

For TPD experiments, the catalyst was cooled in H_2 flow, and CO was adsorbed at 385 K in H_2 flow at either ambient pressure or 2.6 atm. The catalyst was then cooled to 300 K, the carrier gas switched to He, and TPD carried out by raising the catalyst temperature at 1 K/s in He flow.

For most TPR experiments, the catalyst was cooled in H_2 flow from 773 K, and CO was adsorbed at 385 K. In a few experiments the catalyst was cooled from 773 K in He flow, and CO was adsorbed at 300 K in He. The adsorption time was varied for two series of experiments at 385 K; ambient pressure H_2 was used during one adsorption series and H_2 at 2.6 atm was used for the other series. In some cases CO was adsorbed in H_2/He mixtures. Separate mass flow controllers were used for H_2 and He to obtain these mixtures. A back pressure regulator was used to control the total pressure of the reaction system above ambient. For some TPR experiments, the catalyst was exposed to pulses of 100% ^{13}CO for 15 min or 20 min at 300 K after ^{12}CO adsorption in H_2 at 385 K. Masses 15, 17 ($^{13}CH_4$), 28, 29(^{13}CO), 31, 32 ($^{13}CH_3O$), 44, 45, 46, and 47 ($^{13}CH_3OCH_3$) were monitored during the subsequent TPR experiment. To obtain the $^{13}CH_4$ spectra, the mass 17 signal was corrected for cracking of H_2O. The TPR experiments were carried out by raising the catalyst temperature at a rate of 1 K/s in *ambient pressure* H_2 flow, regardless of the adsorption pressure.

The procedure used to prepare the Pd/Al_2O_3 catalyst was adapted from Palazov *et al.* (*11*). Kaiser A-201 alumina (60 to 80 mesh) was impregnated to incipient wetness with aqueous $PdCl_2$. The impregnated alumina was air-dried for 24 h and then dried in vacuum for 24 h at 373–383 K. The catalyst was then calcined for 10 min at 573 K with 2% O_2 in N_2, reduced in H_2 at 573 K

for 5 h, and finally passivated with 2% O_2 in N_2 at room temperature. This catalyst had a weight loading of 3.7% Pd, as measured by ICP-MS. Because this catalyst showed signs of incomplete reduction during preliminary experiments, it was further reduced for 5 h at 773 K.

Miura *et al.* (*19*) reported that chlorine has little or no effect on the chemisorption capacity or the propane hydrogenolysis rate for Pd/Al_2O_3 catalysts reduced at 600 K. They concluded that most of the chlorine remaining from the catalyst preparation was associated with the support, not the Pd. Since our studies involve CH_3O adsorbed on the support, this chlorine might be expected to affect CH_3O adsorption, but the CH_3O amounts we observe are similar to those seen on Ni/Al_2O_3 catalysts that do not contain chlorine.

RESULTS AND DISCUSSION

Identification of CH_xO Species

As observed previously for Ni, Ru, and Pt supported on Al_2O_3 (*6, 8, 20*), when CO was adsorbed for 30 min on Pd/Al_2O_3, more CO adsorbed at 385 K in H_2 flow than at 300 K in He flow. This increase in adsorption amount is not likely to be due to carbon deposition at 385 K; several studies have reported that CO does not dissociate to a significant extent below 475 K on Pd (*11, 17*), and CO desorbs from Pd/Al_2O_3 with very little CO_2 formation. Ichikawa *et al.* (*21*) reported that CO disproportionated on highly-dispersed Pd/SiO_2 catalysts, but for a lower dispersion of 45%, CO did not disproportionate. Thus, significant carbon deposition is not expected on our catalysts.

After CO adsorption at 385 K in H_2 flow, H_2 and CO desorbed simultaneously, with a peak maximum at 495 K, during a subsequent TPD. The H_2 and CO desorption peaks were quite different from those observed when H_2 and CO were adsorbed individually on this catalyst or other Pd/Al_2O_3 catalysts (*14, 15*). Because of these differences and because H_2 and CO desorbed simultaneously, their formation during TPD was concluded to be limited by decomposition of a CH_xO surface species. The H/CO ratio was 3.8. The similarity of the TPD results to previous TPD studies on other Al_2O_3-supported metals (*6, 8, 20*), and the detection of CH_3O on Pd/Al_2O_3 by infrared spectroscopy (*11*) indicates that CH_3O may be present on our Pd/Al_2O_3 catalyst. The CH_3O is most likely adsorbed on the Al_2O_3 surface, since studies with mixtures of Al_2O_3 and Pt/Al_2O_3 (*8*) and Al_2O_3 and Ni/Al_2O_3 (*22*) show that CH_3O is on the Al_2O_3. The infrared studies by Palozov *et al.* (*11*) also concluded that CH_3O was on the Al_2O_3 support. They concluded CH_3O formed on Pd and was subsequently transferred to Al_2O_3 by spillover (*11*). An exact measure of the stoichiometry of the adsorbed CH_xO species cannot be determined from the TPD amounts because H_2 and CO are also adsorbed on the Pd surface. Small amounts of CH_4 and CO_2 (less than 2% of the CO amount) were also observed during TPD of coadsorbed CO and H_2, but no CH_3OH desorbed.

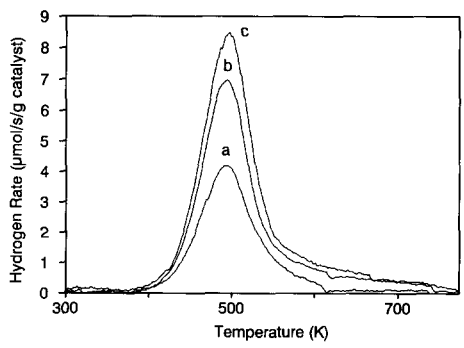

FIG. 1. Hydrogen TPD spectra following CO and H_2 coadsorption at 385 K on 3.7% Pd/Al_2O_3. The H_2 carrier gas was at 2.6 atm and CO pulses were injected for (a) 15 min, (b) 30 min, (c) 60 min.

Temperature-programmed desorption was also carried out following CO adsorption in 2.6 atm H_2 for various times. As observed for CO adsorption in H_2 flow at ambient pressure, CO and H_2 desorbed simultaneously, with a peak maximum at 495 K (Figs. 1 and 2). Figures 1(a) and 2(a) (CO

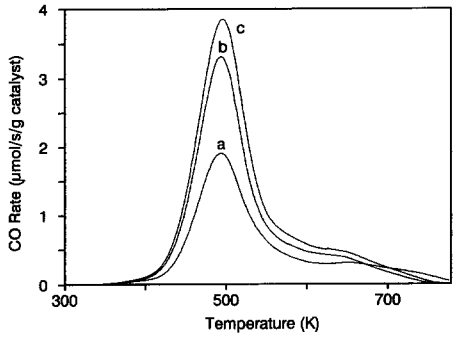

FIG. 2. Carbon monoxide TPD spectra following CO and H_2 coadsorption on 3.7% Pd/Al_2O_3. Same conditions as Fig. 1.

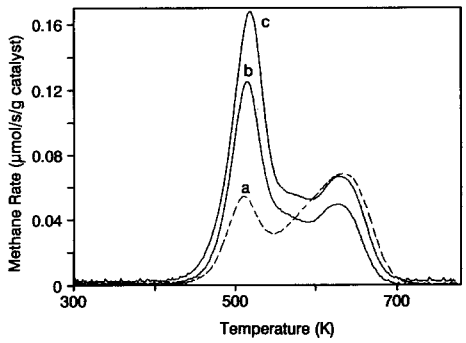

FIG. 3. Methane TPD spectra following CO and H_2 coadsorption on 3.7% Pd/Al_2O_3. Same conditions as Fig. 1.

adsorption for 15 min in 2.6 atm H_2) are almost identical to the H_2 and CO spectra observed following CO adsorption in ambient pressure H_2 for 30 min. The stoichiometry of the CH_xO species was estimated from the H/CO ratio, which was 3.3 when the CH_4 and CO_2 amounts were taken into account. The H/CO ratio of the amplitudes of the TPD peaks at 495 K was 4.5. When the CO adsorption time was increased from 15 to 30 min in 2.6 atm H_2, the H_2 and CO desorption amounts increased significantly (Figs. 1(b) and 2(b)), and the H/CO ratio increased to 3.6. When CO exposure in 2.6 atm H_2 was increased from 30 to 60 min, the amount of adsorbed CO only increased by 15%; the surface was close to saturation after 60 min exposure. The H/CO ratio was 3.8. These stoichiometric values are consistent with the formation of CH_3O, which has been observed by infrared spectroscopy. However, some CH_3OH and CH_3OCH_3 may also have formed, particularly at the higher exposures. For convenience we will refer to the CH_xO species as CH_3O.

During TPD, CH_4 formed in two distinct peaks, as shown in Fig. 3. The amount of CH_4 is small; note the scale difference beteen Figs. 2 and 3. The site responsible for the high-temperature CH_4 peak appears to saturate first, at low exposures. Small amounts of CO_2 were also observed. Desorption of methanol and dimethyl ether during TPD was only detected in trace amounts following the 60-min adsorption experiment. Thus, the CH_3O species readily decomposed to mostly CO and H_2.

Hydrogenation of Adsorbed Carbon Monoxide

To compare CO and CH_3O hydrogenation, CO was first adsorbed at 300 K in He flow, since this should ensure that initially the CO is present only on the Pd surface. Subsequent hydrogenation of this adsorbed CO yielded almost exclusively CH_4, in what appears to be two overlapping peaks, as shown in Fig. 4(a). The overall peak maxi-

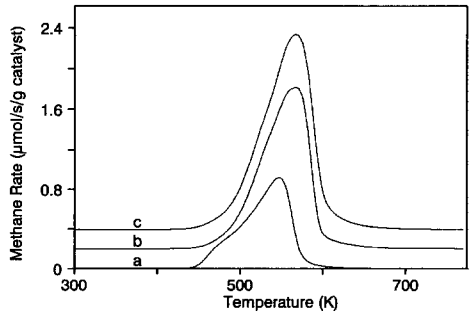

FIG. 4. Methane TPR spectra on 3.7% Pd/Al_2O_3. Carbon monoxide adsorption conditions (a) He flow, 30 min at 300 K; (b) ambient pressure H_2 flow, 30 min at 385 K; (c) ambient pressure H_2 flow, 60 min at 385 K. Note that the curves are displaced vertically for clarity.

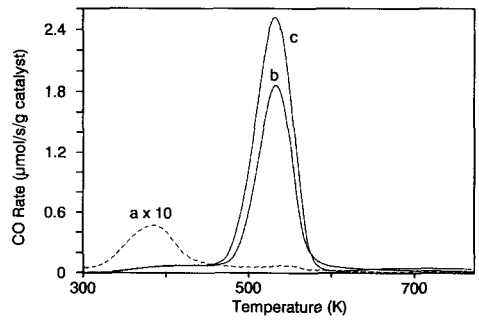

FIG. 5. TPR spectra of unreacted CO on 3.7% Pd/Al_2O_3. Same conditions as Fig. 4.

mum was at 545 K, and reaction was complete by 600 K. Most of the unreacted CO (5% of the CH_4 amount) desorbed below 450 K, as shown in Fig. 5(a). When the catalyst was cooled in H_2 flow from 773 K and CO was adsorbed in H_2 at 300 K, the CH_4 and CO TPR spectra were the same as those in Fig. 4(a) and 5(b), respectively. Since the CO essentially adsorbed only on the Pd surface at 300 K in He flow, the CH_4 + CO amounts formed during TPR were used to estimate a Pd dispersion of 20%. This is a good estimate of dispersion because in other studies good agreement was obtained between TPR and H_2–O_2 titration on a Pd/SiO_2 catalyst (*12*).

Though the CO was adsorbed on Pd at 300 K in He, CH_3O or its precursor spills over onto the Al_2O_3 during TPR to form adsorbed CH_3O. This spillover process was identified on Ni/Al_2O_3 and Ni/TiO_2 catalysts by isotope labeling, and similar experiments on Pd/Al_2O_3 are presented in a later section of this paper. Two distinct CH_4 peaks due to CH_3O and CO hydrogenation could not be identified on Pd/Al_2O_3, however. The heating rate was decreased from 1.0 K/s to 0.1 K/s in an attempt to distinguish two distinct CH_4 peaks, but this approach was not successful. The shape of the CH_4 spectrum did not change at the lower heating rate; the methanation rate decreased by a factor of 10 and the main CH_4 peak shifted to 492 K.

To study CH_3O hydrogenation, CO and H_2 were coadsorbed at 385 K since TPD experiments showed that this procedure produced CH_3O. Three times more CO adsorbed on Pd/Al_2O_3 at 385 K in H_2 than at 300 K in He. However, in contrast to Ni/Al_2O_3 catalysts, only half of this adsorbed CO (present as CH_3O and CO) was hydrogenated to CH_4. The other half desorbed as CO, as shown in Fig. 5(b). The amount of CH_4 formed (Fig. 4(b)) approximately doubled upon adsorption at 385 K, and the CH_4 peak temperature increased by 25 K. Methane formed in a broad peak, and the methanation rate below 500 K is *lower* for Fig. 4(b) than for Fig. 4(a). That is, at the higher coverage, the rate of methanation is lower than at a lower initial coverage. The higher coverage of CH_3O appears to inhibit CH_4 formation, perhaps by inhibiting CO spillover from Pd to Al_2O_3. Thus, fewer Pd sites are available for H_2 adsorption at the lower temperature in Fig. 4(b) because CO remains on Pd. For longer CO exposure times, the amount of CH_4 formed during TPR did not increase (Fig. 4(c) is essentially identical to Fig. 4(b), but the amount of unreacted CO increased (Fig. 5(c) is larger than Fig. 5(b). At the higher exposures, small amounts of CH_3OH and CH_3OCH_3 also formed during TPR, as might be expected for high CH_3O coverages.

A comparison of Figs. 2 and 5 shows that CO desorbed with a 38 K higher peak temperature during TPR than during TPD. Carbon monoxide started forming at 400 K during TPD, but the rate of CO formation during TPR was only significant above 475 K. Thus, the CO desorption peaks during TPR were much narrower than those during TPD. Similarly, CH_4 formed with a 73 K higher peak temperature during TPR (Fig. 4(b),(c) than CO did during TPD. That is, for the same initial coverages, the presence of gas phase H_2 significantly delayed CO desorption, most likely by inhibiting CH_3O decomposition.

The high steady-state methanation activity of Pd/Al_2O_3, relative to Pd/SiO_2 or un-

supported Pd, may result because CH_3O on Pd/Al_2O_3 is hydrogenated faster than CO on Pd. For CO adsorbed at 300 K on Pd/Al_2O_3, some of the CO was hydrogenated to CH_4 during TPR starting at 450 K, with a shoulder below 500 K. The peak temperature was 545 K, and 95% of the adsorbed CO was hydrogenated to CH_4. On Pd/SiO_2, Rieck and Bell (*12*) observed a CH_4 peak temperature of 635 K, and only 43% of the CO adsorbed at 300 K was hydrogenated to CH_4. Thus, the TPR results are consistent with steady-state kinetics, where the rate of methanation has been reported to be 35 times higher on Pd/Al_2O_3 than on Pd/SiO_2 (*10*). As the CH_3O coverage was increased by CO and H_2 adsorption at 385 K, the rate of methanation below 500 K decreased and the CH_4 peak temperature increased. Even under these conditions, however, the CH_4 peak temperature on Pd/Al_2O_3 is much lower than that for Pd/SiO_2 (*12*).

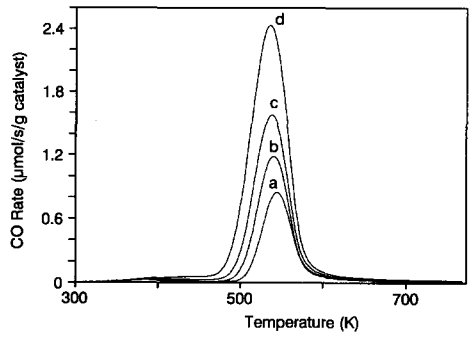

FIG. 6. Carbon monoxide TPR spectra on 3.7% Pd/Al_2O_3. The TPR was carried out in ambient pressure H_2 (0.82 atm) but CO was adsorbed for 30 min at 385 K at a H_2 pressure of (a) 0.20 atm, (b) 0.41 atm, (c) 0.82 atm, (d) 2.6 atm.

Effect of H_2 Pressure on Adsorption

The increased coverage with adsorption temperature and exposure time observed during TPR experiments is consistent with the TPD experiments. Thus, at higher coverages much of the CH_3O does not hydrogenate to CH_4 during TPR. To study this, CO was adsorbed at 385 K for 30 min in various H_2 partial pressures. Temperature-programmed reaction was then carried out in each case in ambient pressure H_2. For a 13-fold change in H_2 pressure during adsorption (from 0.2 to 2.6 atm), the amount of CH_4 formed during TPR changed only slightly. Approximately 135 ± 15 μmol CH_4/g catalyst formed in each case, and the CH_4 spectra were almost the same as the CH_4 spectrum in Fig. 4(b).

In contrast to the CH_4 amounts, the amount of unreacted CO increased significantly as the H_2 pressure increased, as shown in Fig. 6. For the same 13-fold change in H_2 pressure during adsorption, the CO signal increased more than a factor of 3.2. The CO desorption spectra broadened on the low temperature side as the amount of unreacted CO increased. Carbon dioxide production, though small, also increased with H_2 adsorption pressure. Methanol and CH_3OCH_3 were only observed following CO adsorption in 2.6 atm H_2.

The initial rate of spillover to form CH_3O is rapid and does not exhibit much dependence on H_2 pressure. Apparently the concentration of surface hydrogen does not limit the formation of CH_3O at low coverages. As the rate of CH_3O formation decreases at high coverages, the hydrogen coverage starts to affect the rate and thus higher H_2 pressures increase the rate. Moreover, at low coverages, most of the CH_3O is hydrogenated to CH_4 during TPR, but as the coverage increases the fraction of CH_3O that is hydrogenated decreases significantly. These changes with coverage could be due to the formation of two types of CH_3O, perhaps linear and bridged forms as observed by IR for CH_3OH adsorption on Pd/ThO_2 (*23*). However, only one form of CH_3O has been observed by IR on Al_2O_3, and no unreactive CH_3O was detected on Ni/Al_2O_3 (*2*). Thus, the relative rates of CH_3O decomposition versus CH_3O methanation may depend on the CO and H_2 coverages on Pd. As the CH_3O coverage increases, the amount of hydrogen adsorbed on Pd decreases because of coadsorbed CO, and decomposi-

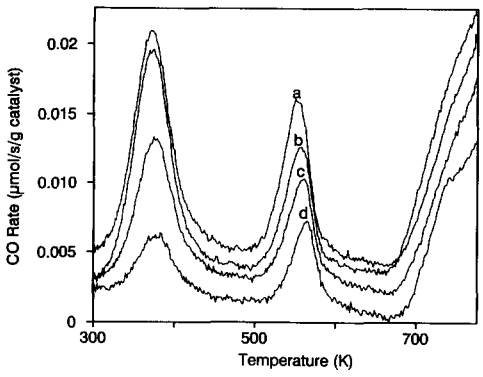

FIG. 7. Carbon monoxide TPR spectra on 3.7% Pd/Al_2O_3. The TPR was carried out in ambient pressure H_2, but CO was adsorbed for 5 min at 385 K in a H_2 pressure of (a) 0.20 atm, (b) 0.41 atm, (c) 0.82 atm, (d) 2.6 atm. Note that the curves are displaced vertically for clarity.

tion competes effectively with methanation. Thus, some CH_3O must decompose and the product CO desorb to obtain a lower coverage so that methanation can take place.

When the same series of adsorption and TPR experiments was carried out for 5 min of CO exposure at 385 K instead of 30 min, less CH_4 was observed during TPR than for 30 min of CO exposure, and the dependence on H_2 pressure during adsorption was still small. When 0.2 atm H_2 was used during adsorption, 69 μmol CH_4/g catalyst formed; for 2.6 atm, 85 μmol CH_4/g catalyst formed. At this lower CO exposure, the amount of unreacted CO observed during TPR was quite small, only 2–3 μmol/g catalyst; the rate of CH_3O formation is rapid at low coverages, and thus H_2 pressure does not affect it much. As shown in Fig. 7, CO desorbed in three distinct peaks, and *less* CO desorbed as the H_2 pressure increased. The high temperature peak is also similar to CO desorption (carbon–oxygen recombination) observed for TPD following CO adsorption at 300 K.

Surface Coverage Variation

The changes in product amounts with CO exposure was studied in 2.6 atm H_2 in order to saturate the surface with CH_3O more rapidly, and adsorption times up to 90 min were used. Since CH_3OH and CH_3OCH_3 were only detected in significant amounts for CO adsorption in 2.6 atm H_2, these conditions also provided a means to obtain higher coverages of oxygenates.

Figure 8 shows the CH_4 and H_2O spectra for three CO exposure times in 2.6 atm H_2 at 385 K. Note that the CH_4 and H_2O signals did not change much (Fig. 8(b),(c)) after the first 15 min of CO exposure (Fig. 8(a)). Note also that H_2O did not appear in the gas phase until CH_4 formation was essentially complete. The H_2O signals were not calibrated, but were presented on a scale consistent with the CH_4 signals. In one experiment, TPR was interrupted at 600 K, a temperature where essentially all the CH_4 and CO had left the surface but the H_2O remained on the Al_2O_3. A subsequent TPR following CO adsorption at 300 K was the same as that in Figs. 4(a) and 5(a). The H_2O at this concentration on the Al_2O_3 did not affect the reaction rate of CO that was originally adsorbed on Pd. The H_2O, which forms as one of the products of the methanation reaction, apparently readsorbs on the Al_2O_3 surface and thus desorbs at a higher temperature than CH_4. Studies on a Ni/SiO_2 catalyst

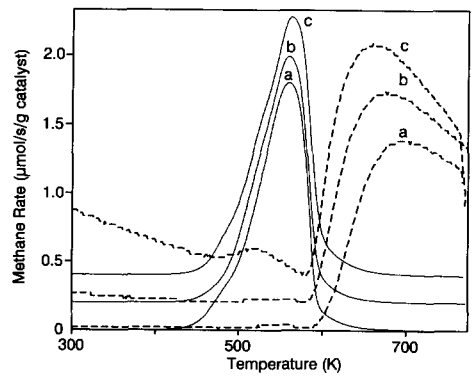

FIG. 8. Methane (solid lines) and water (dashed lines) TPR spectra on 3.7% Pd/Al_2O_3 following CO adsorption at 385 K in 2.6 atm H_2. Carbon monoxide exposure times: (a) 15 min, (b) 30 min, (c) 60 min. Note that the curves are displaced vertically for clarity.

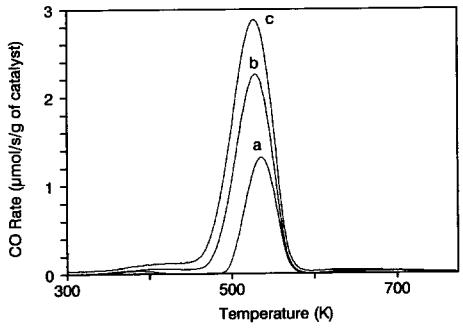

FIG. 9. Carbon monoxide TPR spectra on 3.7% Pd/Al_2O_3. Same conditions as Fig. 8.

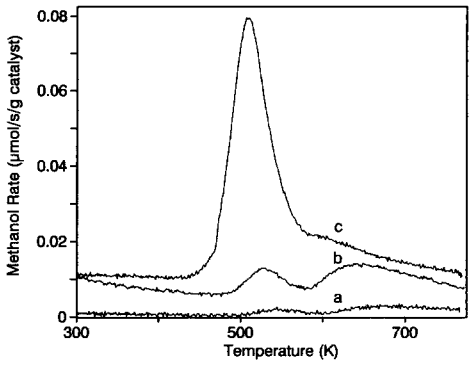

FIG. 10. Methanol TPR spectra on 3.7% Pd/Al_2O_3. Same conditions as Fig. 8. Note that the curves are displaced vertically for clarity.

mixed with an Al_2O_3 support showed that water from methanation, which formed at the same temperature as CH_4 on Ni/SiO_2, was delayed to higher temperatures because of readsorption on Al_2O_3 (*24*).

In contrast to the CH_4 and H_2O signals, the amount of unreacted CO increased at longer exposure times, as shown in Fig. 9. The CH_3OH and CH_3OCH_3 products (Figs. 10 and 11) were barely detectable after 15 min exposure, but these signals exhibited dramatic increases at longer exposure times. A four-fold increase in exposure time increased the concentration of these desorbing oxygenates by 25–100 times. The oxygenate amounts are sensitive to H_2 pressure used during adsorption, even though the CH_4 amount is not. The amount of oxygenates obtained after 15 min of CO exposure at 385 K in 2.6 atm H_2 are almost identical to the amounts obtained after 60 min at 385 K at 0.8 atm H_2, as if the amount of oxygenates increases linearly with H_2 pressure. The CH_3OCH_3 signal had a lower peak temperature than CH_3OH, and its formation was complete by 550 K, but CH_3OH formed in two peaks up to 750 K. The CH_3OH signal was corrected for the cracking fragment from CH_3OCH_3. The ratio of mass 45 to mass 46 signals was used to determine that the signal at mass 46 was from dimethyl ether and not formic acid or ethanol.

The formation of CH_3OH during TPR is consistent with the conclusion that CH_3O forms on the Al_2O_3 surface. Apparently most of the CH_3O either decomposes to CO and H_2 or is hydrogenated completely to CH_4 during TPR. However, near saturation coverage the pathway to CH_3OH desorption opens up. The CH_3OCH_3 may form by CH_3OH decomposition on Al_2O_3 (*25*).

Figure 12 summarizes the amounts of products, observed during TPR, as a function of CO exposure time at 385 K in 2.6 atm H_2. Zero time corresponds to the amounts of products seen for CO adsorption in He at 300 K for 30 min, where all adsorption is expected to be on the Pd surface initially. The total amount of CH_3O adsorption on the Al_2O_3 surface, estimated from the difference

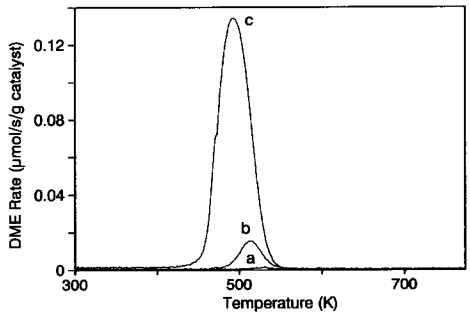

FIG. 11. Dimethyl ether TPR spectra on 3.7% Pd/Al_2O_3. Same conditions as Fig. 8.

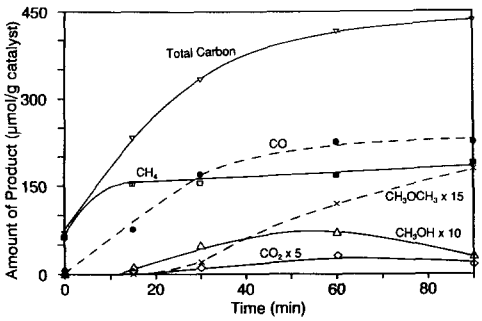

FIG. 12. Product distribution during TPR as a function of CO exposure time. The CO was adsorbed in 2.6 atm H_2 on 3.7% Pd/Al_2O_3 at 385 K.

between the total carbon amounts for adsorption at 385 K for 90 min and 300 K for 30 min, is 360 μmol/g Al_2O_3. This is the same value measured on Ni/Al_2O_3 and on mixtures of Al_2O_3 and Ni/Al_2O_3 (*22*). Since the same Al_2O_3 was used in both studies, the same saturation coverage of CH_3O might be expected to form. Apparently the chlorine that remained on the surface from catalyst preparation did not significantly affect the concentration of CH_3O that formed.

Note in Fig. 12 that the CH_4 amount is essentially saturated after 15 min (or less) exposure, but unreacted CO is only saturated after 60 min exposure. The dimethyl ether signal does not appear to reach saturation, even at 90 min, but dimethyl ether represents a small fraction of the total amount of products. The methanol signal decreased at longer times while dimethyl ether increased, as if the additional adsorption time allowed adsorbed methanol to decompose to dimethyl ether.

Isotope Labeling

In an attempt to study the process that occurred during TPR and to distinguish CO that was originally adsorbed on Pd from CH_3O adsorbed on Al_2O_3, isotopically labeled CO was used. The procedure for these experiments was as follows:

(1) ^{12}CO was adsorbed in H_2 flow at 385 K.

(2) The catalyst was then exposed to ^{13}CO at 300 K in H_2 flow for 20 min.

(3) TPR was carried out and $^{13}CH_4$, $^{12}CH_4$, ^{13}CO, and ^{12}CO were observed.

The objective of Step (1) was to form $^{12}CH_3O$ on the Al_2O_3 surface, and in a series of three experiments a range of $^{12}CH_3O$ coverages was used. Simultaneous with $^{12}CH_3O$ formation, ^{12}CO adsorbed on Pd. The objective of Step (2) was to exchange only the ^{12}CO on Pd with ^{13}CO.

Thus, at the start of the TPR experiment, only $^{12}CH_3O$ was adsorbed on Al_2O_3 and mostly ^{13}CO was adsorbed on Pd. Several results confirmed that this was the starting condition:

- In a separate experiment, ^{13}CO was adsorbed at 300 K for 15 min in He flow. The catalyst was then exposed to ^{12}CO in He flow at 300 K for 15 min. A subsequent TPR experiment yielded mostly $^{12}CH_4$. The $^{13}CH_4$ signal was only 15% of the $^{12}CH_4$ signal, and had the same shape. Similarly, a small amount of unreacted ^{12}CO was detected, and the ^{13}CO signal was only 15% of the ^{12}CO signal. That is, the majority of the ^{13}CO, which was adsorbed on Pd, exchanged with gas phase ^{12}CO at 300 K in 15 min.
- The $^{12}CH_3O$, which formed in Step (1), is not expected to exchange with gas phase ^{13}CO in Step (2) because $^{12}CH_3O$ on the Al_2O_3 surface of Ni/Al_2O_3 did not exchange with ^{13}CO (*26*).
- The combined amounts of ^{13}CO and $^{13}CH_4$ measured in each of the TPR experiments described below was approximately the same as that observed when CO was adsorbed only at 300 K. That is, even when $^{12}CH_3O$ was present on Al_2O_3, ^{13}CO was only adsorbed (by exchange) on the Pd surface.

When no adsorption was carried out at 385 K (Step (1)), and ^{13}CO (or ^{12}CO) was adsorbed on Pd/Al_2O_3 at 300 K, 95% of the CO reacted to CH_4 during TPR (Figs. 4(a) and 5(a)). However, as the amount of $^{12}CH_3O$ increased (by longer ^{12}CO exposure

TABLE 1

^{13}CO Hydrogenation during TPR for Isotope Labeling Experiments

^{12}CO adsorption conditions	Percentage of ^{13}CO hydrogenated to $^{13}CH_4$
No ^{12}CO adsorption (Fig. 4a, 5a)	95
20 min at 385 K in ambient H_2 (Fig. 13)	60
30 min at 385 K in ambient H_2	42
60 min at 385 K in 2.6 atm H_2 (Fig. 14)	14

at 385 K or higher H_2 pressures in Step (1)) the percentage of ^{13}CO that was hydrogenated to $^{13}CH_4$ decreased dramatically, as shown in Table 1.

Figure 13 shows the TPR spectra obtained when ^{12}CO was adsorbed for 20 min at 385 K in Step (1). The $^{12}CH_4$ and ^{12}CO result from the adsorbed $^{12}CH_3O$. The $^{13}CH_4$ signal was similar in shape to the $^{12}CH_4$ signal. Only 60% of the adsorbed ^{13}CO was hydrogenated to $^{13}CH_4$. Some of the ^{13}CO desorbed below 475 K, as observed in Fig. 5(a). However, the majority of the unreacted ^{13}CO desorbed above 475 K; the rate

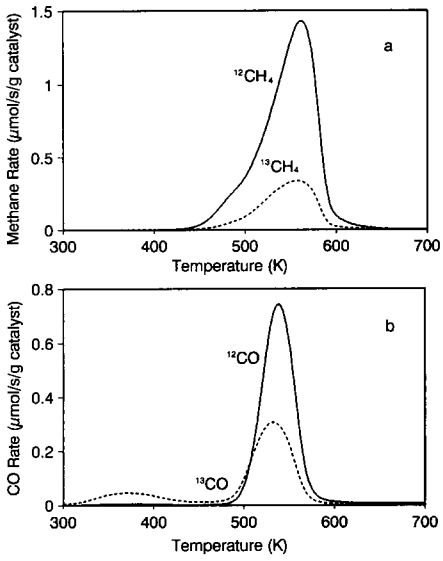

FIG. 13. TPR spectra for ^{12}CO adsorption at 385 K in ambient pressure H_2 for 20 min followed by 20 min of ^{13}CO exposure in ambient pressure H_2 at 300 K: (a) $^{12}CH_4$ and $^{13}CH_4$, (b) ^{12}CO and ^{13}CO.

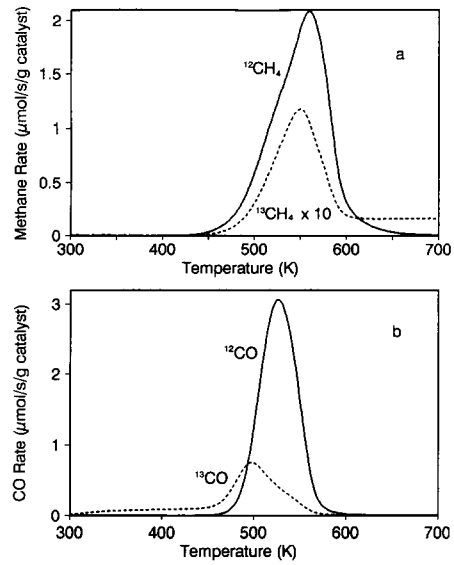

FIG. 14. TPR spectra for ^{12}CO adsorption at 385 K in 2.6 atm H_2 for 60 min followed by 20 min of ^{13}CO exposure in ambient pressure H_2 at 300 K: (a) $^{12}CH_4$ and $^{13}CH_4$, b) ^{12}CO and ^{13}CO.

of ^{13}CO desorption above 475 K in Fig. 13 is 65 times that observed in Fig. 5(a). Note that ^{13}CO desorbed with a lower peak temperature than ^{12}CO.

As the $^{12}CH_3O$ coverage increased, the changes in the ^{13}CO desorption and hydrogenation continued. As shown in Fig. 14, at close to saturation $^{12}CH_3O$ coverage, only 14% of the adsorbed ^{13}CO was hydrogenated to $^{13}CH_4$. Moreover, ^{13}CO desorbed at a significantly lower temperature than ^{12}CO. The ^{13}CO peak temperature is 495 K and that of ^{12}CO is 526 K. Figure 14 also shows that CH_3O on Al_2O_3 is more likely to be hydrogenated than CO on Pd.

The large changes in the desorption and hydrogenation properties of ^{13}CO adsorbed on Pd are the result of the spillover processes that take place during TPR. At low initial $^{12}CH_3O$ coverages, ^{13}CO, which was originally on Pd, formed $^{13}CH_3O$ on Al_2O_3 by spillover during TPR, and this $^{13}CH_3O$ was subsequently hydrogenated almost completely to $^{13}CH_4$. At high initial $^{12}CH_3O$ coverages, the methanation probability de-

creased, as shown. Thus, the majority of the ^{13}CO, which was adsorbed on Pd, may have desorbed directly from Pd. As seen in Fig. 9, as the CH_3O coverage increased, CO desorbed at progressively lower temperatures. The higher CH_3O coverage may have provided a driving force for $^{12}CH_3O$ to diffuse back to Pd at high temperatures and this could have increased the rate of ^{13}CO deposition from the Pd (*16*). Figures 13 and 14 show that the CO adsorbed on Pd preferentially desorbed at lower temperatures.

Thus, the TPR experiments with isotopes show that CO is hydrogenated on Pd/Al_2O_3 by first spilling over onto the Al_2O_3 to form CH_3O. The CH_3O then hydrogenates faster than CO on Pd.

Mechanism

A mechanism in which CO is not dissociated to carbon and oxygen but the CO molecule is first partially hydrogenated was proposed by Mori *et al.* (*27, 28*) for Pd/Al_2O_3. They proposed that a H_2COH intermediate was formed on the Pd surface. A process in which CO is partially hydrogenated before dissociating is consistent with our observation that CH_3O is hydrogenated faster than CO on Pd. This may explain the higher methanation activity of Pd/Al_2O_3 relative to Pd/SiO_2, since CH_3O forms on Al_2O_3 surfaces from $CO + H_2$ but not on SiO_2 surfaces for Pd catalysts (*11*). Vannice *et al.* (*29*) proposed that the support facilitated bond rupture and was directly involved in the methanation process. They also concluded that the support is directly involved in methanol synthesis.

The hydrogenation of CH_3O, which is adsorbed on the support, may be the dominant reaction for methanation on Pd/Al_2O_3. This may not be the pathway for methanol formation, however, since the rate of methanol formation was similar for Pd/SiO_2 and Pd/Al_2O_3 (*17*). Similarly, Pd/La_2O_3 is more active for methanation than Pd/SiO_2, and the rate expressions for methanation on the two catalysts are different (*30*). Also, following CO adsorption at 300 K, the peak temperature during TPR was 525 K for Pd/La_2O_3 and 635 K for Pd/SiO_2 (*12*). While only 43% of adsorbed CO on Pd/SiO_2 was hydrogenated to CH_4, 94% of CO on Pd/La_2O_3 was hydrogenated (*12*). That is, Pd/La_2O_3 and Pd/Al_2O_3 exhibited similar behavior, and CH_3O hydrogenation may be responsible for the higher activity of Pd/La_2O_3. However, the rate expressions for methanol synthesis are similar for Pd/SiO_2 and Pd/La_2O_3, which indicates the mechanism for methanol synthesis is the same on these catalysts (*30*).

CONCLUSIONS

On Pd/Al_2O_3, CH_3O species readily form on the Al_2O_3 surface from CO and H_2 in an activated process. At low coverages, CH_3O is readily hydrogenated to CH_4, but at high CH_3O coverages decomposition and desorption compete with methanation. The CH_3O coverage increases with H_2 pressure and exposure time, and the saturation coverage on Al_2O_3 is 360 μmol/g Al_2O_3. Both CH_3OH and CH_3OCH_3 are detected during TPR following CO adsorption at higher H_2 pressures. Isotope studies demonstrated that CO adsorbed on Pd spills over onto Al_2O_3, and the CH_3O on Al_2O_3 is hydrogenated at a faster rate than CO on Pd. Thus, the CH_3O species on Pd/Al_2O_3 hydrogenates at a much faster rate than CO on Pd/SiO_2, and it is possible that CH_3O hydrogenation is responsible for the higher methanation activity observed in steady-state experiments on Pd/Al_2O_3.

ACKNOWLEDGMENTS

We gratefully acknowledge support by the National Science Foundation, grant CBT-8616494, and E. C. H. thanks the Academy of Applied Sciences for support in the preliminary stages of this work. We are grateful to Baoshu Chen for carrying out experiments presented in Figs. 13 and 14. We thank Professors Robert L. Sani and R. Igor Gamow for helping make this research possible. We also thank Dr. Keith B. Kester and Mr. Raymond L. Flesner for useful suggestions and discussions.

REFERENCES

1. Kester, K. B., and Falconer, J. L., *J. Catal.* **89,** 380 (1984).

2. Glugla, P. G., Bailey, K. M., and Falconer, J. L., *J. Phys. Chem.* **92,** 4474 (1988).
3. Bailey, K. M., Chai, G-Y., and Falconer, J. L., *in* "Proceedings, 9th International Congress on Catalysis, Calgary, 1988" (M. J. Phillips and M. Ternan, Eds.), Vol. 3, p. 1090. Chem. Institute of Canada, Ottawa, 1988.
4. Sen, B., and Falconer, J. L., *J. Catal.* **117,** 404 (1989).
5. Sen, B., and Falconer, J. L., *J. Catal.* **122,** 68 (1990).
6. Sen, B., and Falconer, J. L., *J. Catal.* **113,** 444 (1988).
7. Robbins, J. L., and Marucchi-Soos, E., *J. Phys. Chem.* **93,** 2885 (1989).
8. Flesner, R. L., and Falconer, J. L., in preparation.
9. Mao, T-F., and Falconer, J. L., *J. Catal.* **123,** 443 (1990).
10. Vannice, M. A., and Garten, R. L., *Ind. Eng. Chem. Prod. Res. Dev.* **18,** 186 (1979).
11. Palazov, A., Kadinov, G., Bonev, Ch., and Shopov, D., *J. Catal.* **74,** 44 (1982).
12. Rieck, J. S., and Bell, A. T., *J. Catal.* **96,** 88 (1985).
13. Leary, K. J., Michaels, J. N., and Stacy, A. M., *Langmuir* **4,** 1251 (1988).
14. Paryjczak, T., Farbotko, J. M., and Zielinski, P. A., *Pol. J. Chem.* **62,** 567 (1988).
15. Kokh, I. G., Vozdvizhenskii, V. F., and Babenkova, L. V., *Russ. J. Phys. Chem. Engl. Transl.* **63,** 539 (1989).
16. Guo, X., Xu, Y., Zhai, R., Zhu, K., and Huang, J., *Pure Appl. Chem.* **60,** 1307 (1988).
17. Poutsma, M. L., Elek, L. F., Ibarbia, P. A., Risch, A. P., and Rabo, J. A., *J. Catal.* **52,** 157 (1978).
18. Falconer, J. L., and Schwarz, J. A., *Catal. Rev. Sci. Eng.* **25,** 141 (1983).
19. Miura, H., Hondou, H. Sugiyama, K., Matsuda, T. and Gonzales, R. D., *in* "Proceedings 9th International Congress on Catalysis, Calgary, 1988" (M. J. Phillips and M. Ternan, Eds.) Vol. 3, p. 1307. Chem. Institute of Canada, Ottawa, 1988.
20. Glugla, P. G., Bailey, K. M., and Falconer, J. L., *J. Catal.* **115,** 24 (1989).
21. Ichikawa, S., Poppa, H., and Boudart, M., *J. Catal.* **91,** 1 (1985).
22. Sen, B., Falconer, J. L., Mao, T-F., Yu, M., and Flesner, R. L., *J. Catal.* **127,** 465 (1990).
23. Montagne, X., Boulet, R., Freund, E., and Lavalley, J. C., *in* "Structure and Reactivity of Surfaces" (C. Morterra, A. Zecchina, and G. Costa, Eds), p. 695. Elsevier, Amsterdam, 1989.
24. Zagli, E., Ph.D. Thesis, University of Colorado, Boulder, 1981.
25. Fujimoto, K., Asami, K., Shikada, T., and Tominaga, H., *Chem. Lett.* **12,** 2051 (1984).
26. Chen, B., Falconer, J. L. and Chang, L., *J. Catal.* **127,** 732 (1991).
27. Niizuma, H., Mori, T., Miyamoto, A., Hattori, T., Masuda, H., Imai, H., and Murakami, Y., *J. Chem. Soc. Chem. Commun.* **10,** 562 (1982).
28. Mori, T., Masuda, H., Imai, H., Miyamoto, A., Niizuma, H., Hatori, T., and Murakami, Y., *Pan-Pac. Synfuels Conf.* **1,** 152, (1982).
29. Vannice, M. A., Sudhakar, and Freeman, M., *J. Catal.* **117,** 97 (1987).
30. Hicks, R. F., and Bell, A. T., *J. Catal.* **91,** 104 (1985).